# Comparative Study of Microstructural Evolution and Mechanical Properties of Inconel® 718 and Waspaloy® Welds

*Angelos* Kaldellis[1*], *Anastasia* Alexandratou[1], *Anastasios* Kladis[1], *Stavros* Deligiannis[1], *Petros* Tsakiridis[1] and *George* Fourlaris[1]

[1]Lab. of Physical Metallurgy and Center for Electron Microscopy, School of Mining and Metallurgical Engineering, National Technical University of Athens, Heroon Polytechniou 9, 15780 Athens, Greece,

**Abstract.** This research work focuses on the mechanical behaviour comparative assessment in conjunction with microstructural evolution characterization of Waspaloy® and Inconel® 718, following TIG and EB welding. Both of the forth-mentioned alloys are precipitation strengthened Ni-based superalloys, widely used in chemical, petrochemical and aerospace industries. More specifically, Waspaloy® is strengthened by the precipitation of the ordered fcc *gamma prime* intermetallic phase, $\gamma'$ - $Ni_3(Al,Ti)$, while Inconel® 718 is mainly hardened by the ordered bct *gamma double prime* phase, $\gamma''$ - $Ni_3Nb$, in addition to $\gamma'$. After both welding processes, samples of the above superalloys were subjected to appropriate post-weld heat treatment, according to SAE Aerospace Material Specifications. The mechanical response of the tested specimens is assessed via uniaxial tensile tests, combined with fractography. Furthermore, the microstructural characterization of TIG and EB welds is conducted by Scanning Electron Microscopy (SEM), coupled with Energy Dispersive Spectroscopy (EDS), while phase identification was performed through X-Ray Diffraction (XRD). The main objective of the present research work is to examine the influence of post-weld heat treatment on the Waspaloy® and Inconel® EBW and TIG welds microstructural evolution features, correlating them with their corresponding mechanical behaviour.

## 1 Introduction

Waspaloy is strengthened by the precipitation of the intermetallic *gamma prime* phase $\gamma'$ ($Ni_3(Al,Ti)$) and MC, $M_6C$ και $M_{23}C_6$ carbides, while Inconel 718 is mainly strengthened by *gamma double prime* phase $\gamma''$ $(Ni,Co)_3(Nb,Ta,Ti,Al)$, in addition to $\gamma'$ and corresponding carbides. Waspaloy presents some limitations related to its weldability due to its susceptibility to strain age cracking under conditions of heavy restraint and requires special as well as controlled welding conditions [1, 2]. The most widely-used welding process is Tungsten Inert Gas (TIG), a welding technique that uses a non-consumable tungsten electrode. Moreover, Waspaloy is susceptible to welding solidification cracking and during post-weld heat treatment (strain-age cracking). Pre-weld heat treatment, as well as post-weld

* Corresponding author: aggkald@gmail.com

heat treatment, are recommended to avoid failure. The post-weld heat treatment required for Waspaloy to enhance mechanical strength and eliminate internal stresses consists of three stages, namely homogenization, stabilization and ageing [1, 2]. Electron Beam Welding (EBW) is a non-conventional, highly automated and precise technique; suitable for joining materials that are not easily weldable (i.e., Waspaloy) [1, 2].

Inconel 718 is one of the most weldable superalloys, combining very good weldability and machinability with excellent corrosion resistance and mechanical properties, up to 650°C [1, 2]. Inconel 718 was developed to overcome failure (strain age cracking) during welding, attributed to the sluggish precipitation kinetics of the alloy's principal strengthening phase, gamma double prime ($\gamma''$) [1]. Nevertheless, Inconel 718 is susceptible to the formation of the deleterious TCP phase, Laves, due to the segregation of Nb in the interdendritic regions, during solidification. Laves phase is considered a favorable site for crack initiation and propagation, affecting the mechanical properties of the welds, a post-weld heat treatment is suggested [3]. This study aims to investigate the mechanical behaviour of TIG, and EB welded and post-weld heat-treated Ni-based superalloys, Waspaloy and Inconel 718, based on the microstructural characteristics.

## 2 Experimental Procedure

### 2.1 Material Description

Waspaloy (200 mm x 152 mm x 2.22 mm) and Inconel 718 (210 mm x 200 mm x 1.6mm) annealed sheets were used, conformed to SAE Aerospace Material Specifications, AMS 5544J and 5597F, respectively. The nominal chemical composition of both alloys is presented in **Table 1**. Specimens for tensile testing were designed and produced through CNC machining, based on the BS EN 10002-1: 2001 specification, in the case of Waspaloy and ASTM E8/E8M, in the case of Inconel 718.

**Table 1.** Nominal chemical composition of Waspaloy and Inconel 718, according AMS 5828 and AMS 5596.

| | **wt. %** | |
|---|---|---|
| | **Waspaloy** | **Inconel 718** |
| **C** | 0.02-0.10 | <0.08 |
| **Mn** | <0.10 | <0.35 |
| **Si** | <0.10 | <0.35 |
| **P** | <0.10 | <0.015 |
| **S** | <0.10 | <0.015 |
| **Cr** | 18.00-21.00 | 17.00-21.00 |
| **Co** | 12.00-15.00 | <1.00 |
| **Mo** | 3.50-5.00 | 2.80-3.30 |
| **Ti** | 2.75-3.50 | 0.65-1.15 |
| **Al** | 1.20-1.60 | 0.20-0.80 |
| **B** | 0.003-0.010 | <0.006 |
| **Fe** | <2.00 | Balance |
| **Cu** | <0.10 | <0.30 |
| **Zr** | <0.04 | - |
| **Ni** | Balance | 50.00-55.00 |
| **Nb** | - | 4.75-5.50 |
| **Ta** | - | <0.05 |

## 2.2 Welding Processes

### *2.2.1 EB Welding Process*

EB welding process was performed on both Waspaloy and Inconel 718 sheets. The process parameters are presented in **Table 2**.

**Table 2.** EBW process parameters of Waspaloy and Inconel 718 specimens.

| | **Waspaloy** | **Inconel 718** |
|---|---|---|
| **Beam current** | 80 mA | 65 mA |
| **Voltage** | 50 kV | 40 kV |
| **Focusing current** | 7 A | 3.5 A |
| **Travel speed** | 1651 mm/min | |
| **Shielding gas** | Vacuum | |
| **Filler metal** | None (autogenous) | |

### *2.2.2 TIG Welding Process*

TIG welding process was performed on both Waspaloy and Inconel 718 sheets. The process parameters are presented in **Table 3**, as specified by AMS 5828 (Waspaloy) and AMS 5832G (Inconel 718).

**Table 3.** TIG process parameters of Waspaloy and Inconel 718 specimens.

| | **Waspaloy** | **Inconel 718** |
|---|---|---|
| **Welding current** | 80 A | |
| **Voltage** | 14 V | 12 V |
| **Travel speed** | Manual | |
| **Shielding gas** | Argon 99.999% | |
| **Filler metal** | Waspaloy, Ø1.2 | Inconel 718, Ø1.14 |
| **Electrode** | W + 2% Th (EWTh-2), Ø1.6 | W + 2% Th (EWTh-2), Ø1.6 |

## 2.3 Post-Weld Heat Treatment

Post-weld heat treatment (PWHT) was applied to both Waspaloy and Inconel 718 welds (TIG and EB), and more specifically, to the welded tensile test specimens. Concerning the Waspaloy, PWHT is covered within SAE AMS 5544J and consists of three steps, namely the solution treatment at 996°C for 2h, followed by air-cooling, and two-step age-hardening treatment, at 843°C for 4h (stabilization) and 760°C for 16h (precipitation), both followed by air-cooling. Inconel 718 specimens were subjected to a three-step PWHT, according to SAE AMS 5597F, as follows: solution treatment at 1066°C for 1h, followed by air-cooling, two-step ageing, at 760°C for 10h, followed by furnace cooling (first ageing), with a cooling rate of 55°C/h until 649°C, at which second ageing is taken place, for 8h, followed by air-cooling. PWHTs were performed in a protective atmosphere to avoid oxidizing phenomena.

## 2.4 Mechanical Testing (Tensile Testing)

The mechanical properties of the welded and appropriately post-weld heat-treated Waspaloy and Inconel 718 test specimens were assessed, employing tensile testing at room temperature (RT), according to the specification ASTM E8/E8M. An Instron Model 4482 testing machine was used, and the specimens were elongated parallel to the rolling direction and perpendicular to the welding direction, with 1mm/min tensile speed. As already mentioned, the test specimens were designed and manufactured through CNC machining, according to the appropriate specifications; BS EN 10002-1: 2001 (Waspaloy) and ASTM E8/E8M (Inconel 718). **Figure 1a-b** provides the dimensions of the test specimens in each case. It is noted that the specimens were tested after welding and PWHT processes without undergoing any further machining to remove the excess weld metal in the caps of the TIG welds.

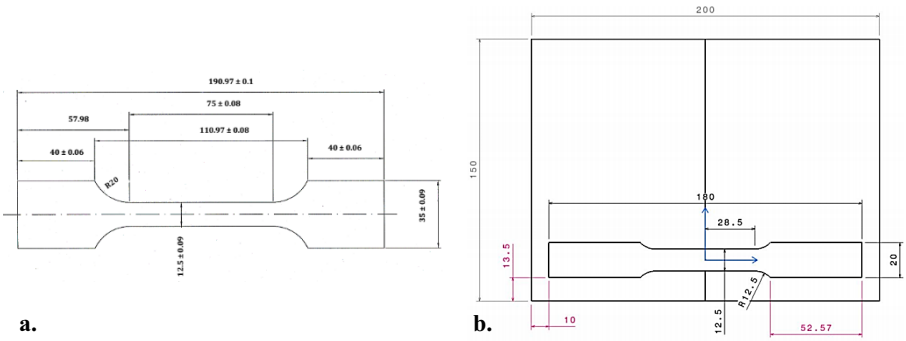


**Fig. 1.** Schematic illustrations of the tensile test specimens of Waspaloy (a) and Inconel 718 (b), providing the specimens' dimensions, measured in mm.

### 2.5 Microstructural Evaluation

Following appropriate metallographic preparation (grinding, polishing and etching with Kalling's No.2 reagent), the microstructural evolution of the Waspaloy and Inconel 718 TIG and EB welds was investigated, employing Scanning Electron Microscopy (SEM-JEOL JSM 6380-LV), coupled with Energy Dispersive Spectroscopy (EDS-INCA X-Sight Oxford Instruments). X-Ray Diffraction analysis system (XRD-Bruker D8 Focus) with an X-Ray source of Cu Kα radiation, operating at 40kV and 40mA, was utilized for phase identification. The scan was performed in the angular range of 30°-55°, with scan speed 0.02°/s, in the case of Waspaloy, and between 10°-110°, with scan speed 0.03°/s, in the case of Inconel 718.

## 3 Results and discussion

### 3.1 SEM and XRD study

The most representative SEM micrographs of Waspaloy and Inconel 718 TIG and EB welds, illustrating the microstructural evolution of each fusion zone (FZ), are provided in **Figures 2-3**. **Figures 4-5** illustrate the characteristics of the fracture surfaces observed in the welded test samples using SEM. **Figure 6** provides the XRD patterns of Waspaloy and Inconel 718 base metal. **Figure 2** shows the FZ microstructure of TIG-welded and PWHTed Waspaloy (**a**) and Inconel 718 (**b**), both consisting of $\gamma$ phase dendrites, characterized by a cruciform structure with non-uniform width and orientation. **Figure 3** shows the FZ microstructure of EB-welded and PWHTed Waspaloy (**a**) and Inconel 718 (**b**).

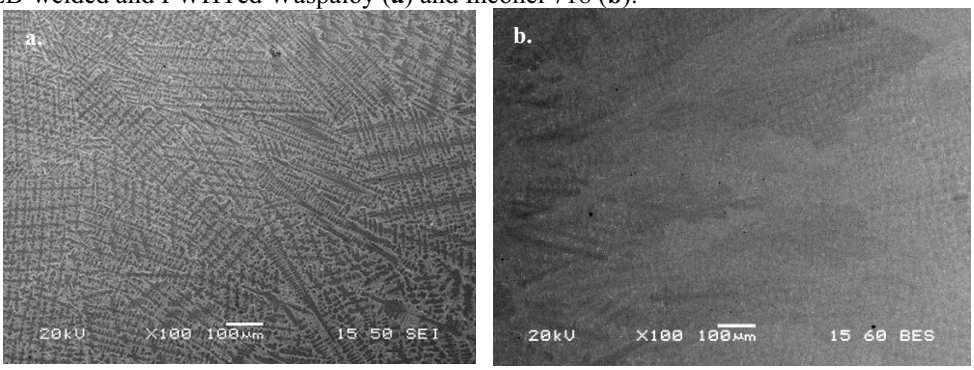


**Fig. 2.** SEM micrographs of Waspaloy (a) and Inconel 718 (b) TIG-welded and PWHTed fusion zone, outlining a cruciform, randomly oriented, $\gamma$ dendritic microstructure and the existence of solidification grain boundaries (SGBs).

Concerning the FZ's microstructural evolution of TIG and EB-welded and PWHTed Waspaloy and Inconel, it is noteworthy that the lower heat input and higher cooling rate of the EB welding process resulted in a considerably finer and columnar $\gamma$ dendritic structure, compared to that of TIG welding process. In the case of EB welding FZs, in both superalloys, the dendritic structure is characterized by a directional growth converging to the weld line. Additionally, dendrites' thickness and arm spacing seem constant, while both are observed wider in the Inconel 718 EB weld FZ. In TIG as-welded Inconel 718, a Nb-rich Laves phase was observed in the FZ's interdendritic regions, which was dissolved following PWHT.

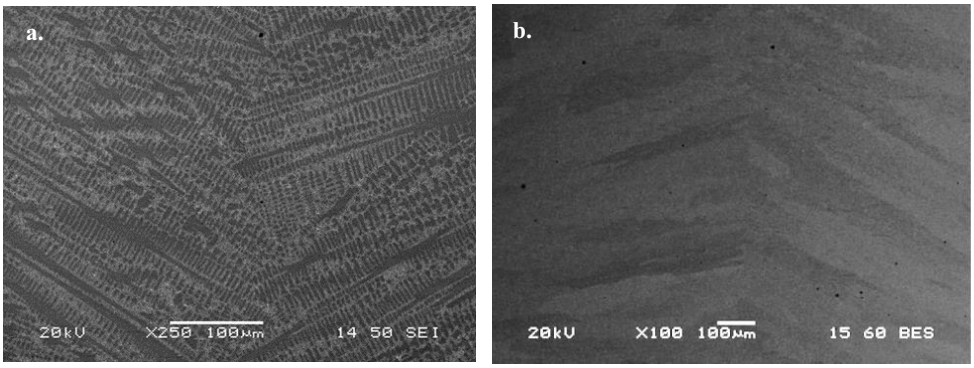


**Fig. 3.** SEM micrographs of Waspaloy (a) and Inconel 718 (b) EB-welded and PWHTed fusion zone, showing the growth of a fine columnar $\gamma$ dendritic structure, oriented to the weld center.

**Figures 4-5** provide representative SEM-SEI micrographs of the fracture surfaces of both superalloys. The EB-welded and PWHTed Waspaloy (**Fig. 4a**) is characterized by a completely detached fracture surface. River patterns and cracks between the cleavage layers are also observed. The TIG-welded and PWHTed Waspaloy fracture surface topography (**Fig. 4b**) reveals the existence of very brittle-fractured regions, along with areas of limited ductility, consisting of dimples. Concerning the EB-welded and PWHTed Inconel 718 fracture surface (**Fig. 5a**), interdendritic fracture with a small percentage of dimples is observed. On the contrary, the TIG-welded and PWHTed Inconel 718 fracture seems more ductile due to the profound dimpled surface; dimples of various sizes and shapes are illustrated in the micrographs.

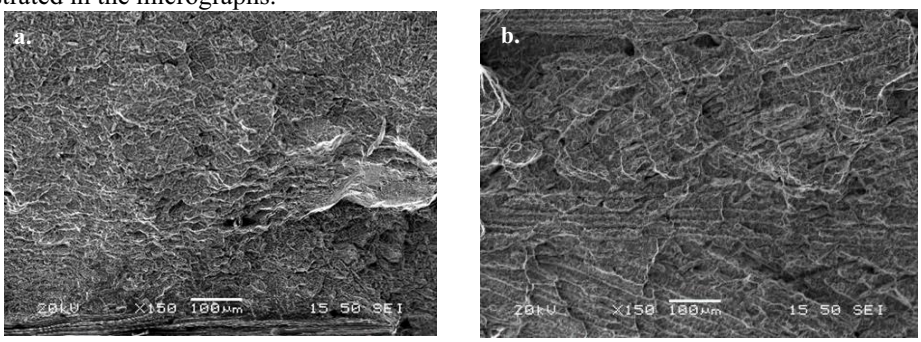


**Fig. 4.** SEM-SEI micrographs, showing the fracture surface of the EB- (a) and TIG-welded (b) and PWHTed Waspaloy samples.

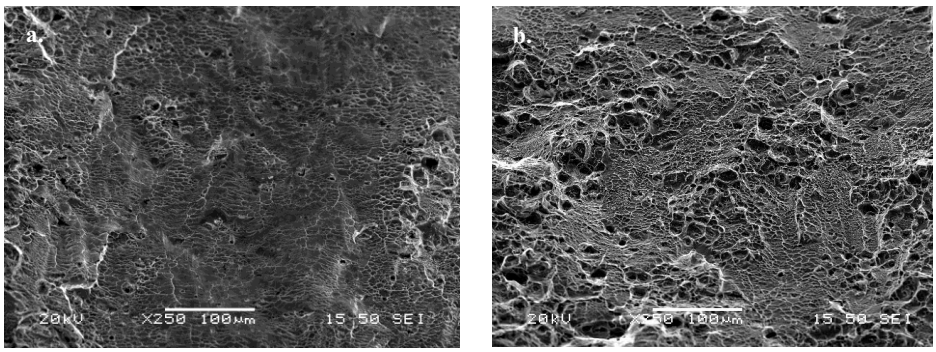


**Fig. 5.** SEM-SEI micrographs, showing the fracture surface of the EB- (a) and TIG-welded (b) and PWHTed Inconel 718 samples.

The phase identification in the heat-treated samples of Waspaloy and Inconel 718 base metals is achieved through XRD analysis (**Fig. 6**). Both superalloys' microstructures consist of the $\gamma'$ phase, primary (MC-type) and secondary ($M_{23}C_6$, $M_6C$-type) carbides dispersed in the $\gamma$-matrix. Deleterious TCP phases (i.e., Laves, σ) are not detected, as they have been dissolved during the PWHT [2-4].

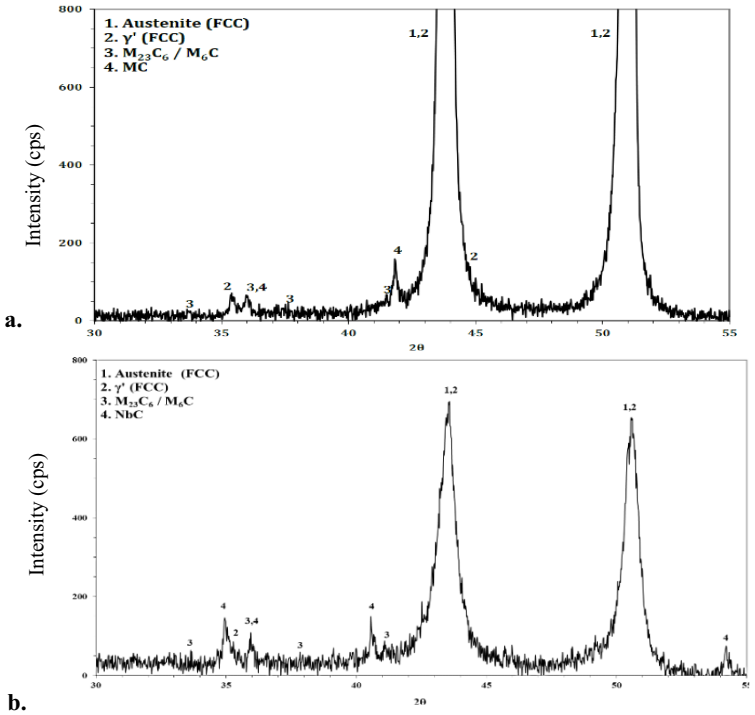


**Fig. 6.** XRD patterns of heat-treated Waspaloy (a) and Inconel 718 (b) base metal.

## 3.2 Tensile Testing

**Figures 7–10** show the stress-strain curves resulting from the tensile testing of the TIG- and EB-welded, and PWHTed Waspaloy (**Fig. 7-8**) and Inconel 718 (**Fig. 9-10**) test specimens. Three specimens were tested per condition. It is of primary importance to note that all welds ruptured at the fusion zone.

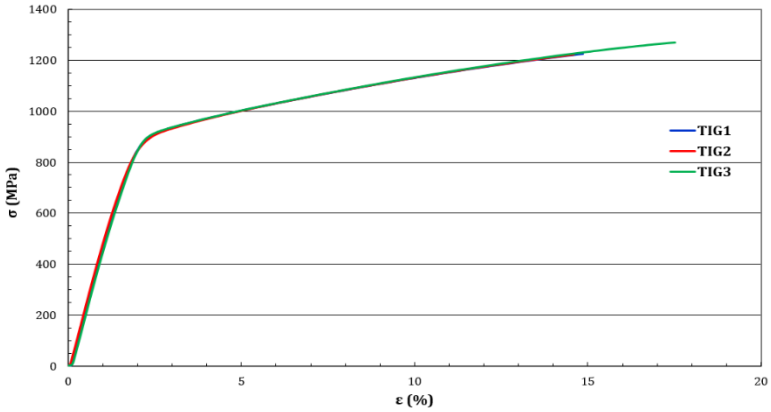


**Fig. 7.** Stress-strain curve of TIG-welded and PWHTed Waspaloy specimens.

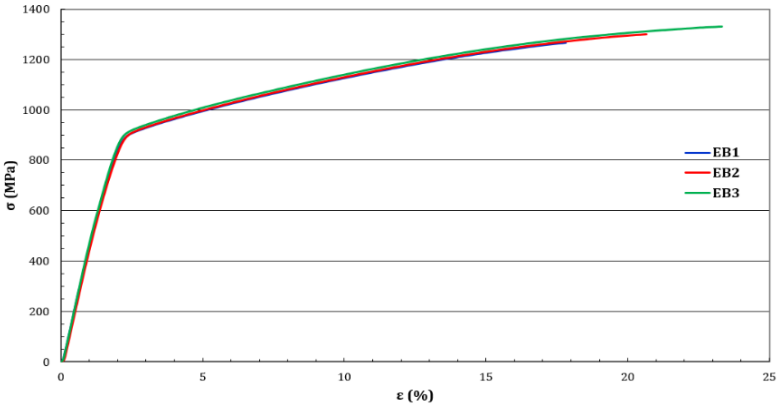


**Fig. 8.** Stress-strain curve of EB-welded and PWHTed Waspaloy specimens.

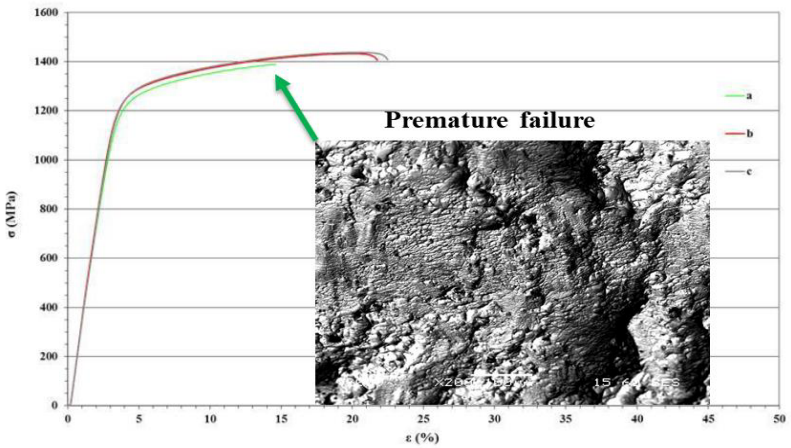


**Fig. 9.** Stress-strain curve of TIG-welded and PWHTed Inconel 718 specimens. SEM-BES micrograph illustrates the fracture surface of the test specimen (premature failure).

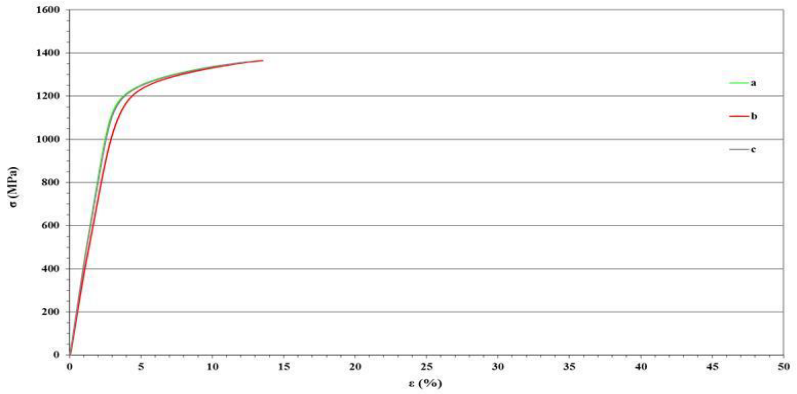


**Fig. 10.** Stress-strain curve of EB-welded PWHTed Inconel 718 specimens.

Based on the stress-strain curves, the mechanical properties of the Waspaloy EB welds are better than those of the TIG welds, as expected. On the other hand, Inconel 718 TIG welds exhibit better mechanical behavior than EB welds. This may be attributed to the sluggish kinetics of Inconel 718 principal strengthening phase ($\gamma''$), which in the case of TIG welding, the lower cooling rate favors its precipitation, thus strengthening the alloy and increasing its ductility [2-4]. The lower heat input and higher cooling rate of EB welding hinder the precipitation of $\gamma''$ in Inconel 718, whereas in Waspaloy promote the development of a fine and fully columnar $\gamma$ dendritic structure in FZ, confirming the tensile testing results. PWHT also plays an essential role in the microstructural evolution and its effect on the welds' mechanical properties.

## 4 Conclusions

The present study, based on microstructural investigation and mechanical testing, highlights the combined effect of TIG and EB welding processes and PWHT on the microstructural evolution, comparing two widely used superalloys, namely Waspaloy and Inconel 718. Waspaloy EB welds exhibit a better mechanical response than TIG ones, whereas Inconel 718 welds have the advert behavior. Furthermore, Waspaloy EB welds are assessed as better than Inconel 718 ones in terms of mechanical strength, while Inconel 718 TIG welds show superior mechanical response than the Waspaloy corresponding ones. The above outcomes conform with the microstructural evaluation. The welding process parameters (heat input, cooling rate), combined with the appropriate PWHT, affect the microstructural features, and consequently, the mechanical strength and ductility of the welds. Microstructural investigation via Transmission Electron Microscopy is suggested in order to further correlate the Waspaloy and Inconel 718 welds' nanostructure to their mechanical behavior.

## References

1. R. C. Reed, The superalloys: fundamentals and applications (Cambridge University Press, 2008).
2. J. Andersson, 9th Int. Symp. on Superalloy 718 & Der.: Energy, Aerospace, and Ind. App. The Min., Met. & Mat. S. (Springer, 2018) doi.org/10.1007/978-3-319-89480-5_60
3. T. Sonar, V. Balasubramaniam, S. Malarvizhi, T. Venkateswaran, D. Sivakumar, Mat. Char., **174**, (2021) doi.org/10.1016/j.matchar.2021.110997.
4. A. Alexandratou, S. Deligiannis, N. Makris, P. Tsakiridis and G. Fourlaris, M&M, **25**, 2 (2019) doi.org/10.1017/S1431927619013916 .